Optimal Pilot Pattern for Time Variant Channels

Michal Šimko, Qi Wang and Markus Rupp

Institute of Telecommunications, Vienna University of Technology, Vienna, Austria
Email: msimko@nt.tuwien.ac.at
Web: http://www.nt.tuwien.ac.at/ltesimulator

***Abstract*—In order to estimate a transmission channel, a typical wireless communications system multiplexes a fixed pattern of symbols known at the receiver within the data-symbols. In Long Term Evolution (LTE), these reference symbols can consume up to 14.2% of the total transmission bandwidth. In this work, we investigate an optimal pilot-symbol pattern design using a post-equalization Signal to Interference and Noise Ratio (SINR) framework. We show how to choose the distance between adjacent pilot-symbols close to optimally and how to distribute the available power among pilot- and data-symbols at the same time under time-variant channels. We confirm our analytical solution by means of simulation. Compared to a system with a fixed distance between pilot-symbols and unit power distribution, the proposed system configuration yields significant gains in terms of capacity.**

***Index Terms*—LTE, Power distribution, OFDM.**

I. Introduction

Coherent detection is widely utilized in current systems for mobile wireless communications. One of the most important aspects of such a system is its pilot-symbol pattern. In this paper, we analyze state-of-the-art knowledge about pilot-symbol patterns under time-variant channels.

A. Related Work

With an increasing amount of wireless communications applications experiencing time-variant channels, also research community addressed more of their contributions towards improvement of such systems. One of the key elements of every coherent wireless communication system is channel estimation that makes use of reference symbols inserted between the data-symbols. In [1, 2], it was shown that equally spaced pilot-symbols are optimal in terms of the channel estimation Mean Square Error (MSE). Authors of [3] chose uncoded Bit Error Ratio (BER) as the optimization criterion for their placement of the pilot-symbols in the time direction. In [4] various approaches for a general pilot-symbol placement are summarized. Cosovic and Auer utilized capacity as the design criterion for pilot-symbols in [5]. However, they used Signal to Interference and Noise Ratio (SINR) approximation valid only for high Signal to Noise Ratio (SNR) values and the utilized model for channel estimation MSE is unnecessary complicated and most importantly, they did not show the amount of pilot-symbols that is an optimal tradeoff between quality of the channel estimates and utilized resources.

Authors of [6–9] showed how to distribute available power among data and pilot-symbols given a certain pilot-symbol pattern. The authors utilized the post-equalization SINR under imperfect channel knowledge as the cost function to solve the formulated problem. This relatively simple framework allows to treat the problem analytically and to find a solution independent of the actual channel realization.

B. Contribution

The main contributions of this paper are:

- We analyze performance of the state-of-the-art channel estimators depending on the maximum Doppler spread.
- We provide analytical expression for the post-equalization SINR including channel estimation error.
- By maximizing the constrained capacity, we derive a close to optimal distance between adjacent pilot-symbols in the time direction depending on the maximum Doppler spread.
- As with our previous work, all data, tools, as well implementations needed to reproduce the results of this paper can be downloaded from our homepage [10].

The remainder of the paper is organized as follows. In Section II, we describe the mathematical system model for transmitting pilots and data over a Multiple Input Multiple Output (MIMO) channel. In Section III, we briefly describe the post-equalization SINR expression for Zero Forcing (ZF) equalizers with imperfect channel knowledge. In Section IV, we summarize our previous work on power distribution between pilot and data-symbols relevant for this work. We formulate the optimization problem for optimal pilot-symbol design in Section V. Finally, we present simulation results in Section VI and conclude our paper in Section VII.

II. System Model

In this section, we briefly introduce a transmission model suitable for our further derivation. A received symbol vector at a discrete time index n transmitted over a flat and time-variant MIMO channel can be written as

$$\mathbf{y}\left[n\right] = \mathbf{H}\left[n\right]\mathbf{W}\mathbf{s}\left[n\right] + \mathbf{n}\left[n\right], \tag{1}$$

where $\mathbf{H}\left[n\right] \in \mathbb{C}^{N_\mathrm{r}\times N_\mathrm{t}}$ represents the MIMO channel matrix at a discrete time index n. The precoding matrix is denoted by $\mathbf{W}$. The transmitted symbol vector is referred to as $\mathbf{s}\left[n\right]$. The vector $\mathbf{n}\left[n\right] \in \mathbb{C}^{N_\mathrm{r}\times 1}$ denotes additive white zero mean Gaussian noise with variance σ_n^2 on antenna n_r. The individual channel coefficients $h_{n_\mathrm{r},n_\mathrm{t}}\left[n\right]$ are spatially uncorrelated and

are generated according to Jakes' model with time autocorrelation function

$$\mathbb{E}\left\{h_{n_{\mathrm{r}},n_{\mathrm{t}}}[n]\, h_{n_{\mathrm{r}},n_{\mathrm{t}}}[n]^{*}\right\} = \mathrm{J}_0\left(2\pi f_d T_s (m-n)\right), \quad (2)$$

where $\mathrm{J}_0(\cdot)$ denotes the zeroth order Bessel function. The variable f_d represents the maximal Doppler frequency and T_s the symbol duration. The maximal Doppler frequency can be obtained by the following expression

$$f_d = \frac{v_{\max} f_c}{c_0}, \quad (3)$$

where $v_{\max}$ is the maximal user velocity, f_c the carrier frequency, and c_0 the speed of light.

We denote the effective channel matrix by

$$\mathbf{G}[n] = \mathbf{H}[n]\,\mathbf{W}[n]. \quad (4)$$

Furthermore, the average power transmitted on each of the N_l layers is denoted by σ_s^2. The power transmitted on each data position is σ_{d}^2, while it is σ_{p}^2 on each pilot position.

III. Post-equalization SINR

In this section, we consider a time-variant scenario and briefly describe an analytical expression for the post-equalization SINR of a MIMO system using a ZF equalizer based on imperfect channel knowledge. More details can be found in our previous work [8].

If perfect channel knowledge is available at the equalizer, the ZF estimate of the data-symbol is given as

$$\hat{\mathbf{s}}[n] = \left(\mathbf{G}[n]^{\mathrm{H}}\mathbf{G}[n]\right)^{-1}\mathbf{G}[n]^{\mathrm{H}}\mathbf{y}[n]. \quad (5)$$

The data estimate $\hat{\mathbf{s}}[n]$ defined in Equation (5) results in a post-equalization SINR of the m-th layer given as [11, 12]

$$\gamma_m = \frac{\sigma_s^2}{\sigma_n^2 \mathbf{e}_m^{\mathrm{H}}\left(\mathbf{G}[n]^{\mathrm{H}}\mathbf{G}[n]\right)^{-1}\mathbf{e}_m}, \quad (6)$$

where the vector $\mathbf{e}_m$ is an $N_{\mathrm{l}} \times 1$ zero vector with a one on the m-th element. This vector extracts the signal on the corresponding layer m after the equalizer.

Let us proceed to the case of imperfect channel knowledge. We define the perfect channel as the channel estimate plus the error matrix due to the imperfect channel estimation

$$\mathbf{H}[n] = \hat{\mathbf{H}}[n] + \mathbf{E}[n], \quad (7)$$

where the elements of the matrix $\mathbf{E}[n]$ are random variables, statistically independent of each other with zero mean and variance σ_e^2. Inserting Equation (7) in Equation (1), the input-output relation changes to

$$\mathbf{y}[n] = \left(\hat{\mathbf{H}}[n] + \mathbf{E}[n]\right)\mathbf{W}[n]\,\mathbf{s}[n] + \mathbf{n}[n]. \quad (8)$$

Since the channel estimation error matrix $\mathbf{E}[n]$ is unknown at the receiver, the ZF solution is given again by Equation (5), but channel matrix $\mathbf{H}[n]$ is replaced by its estimate $\hat{\mathbf{H}}[n]$, which is known at the receiver

$$\hat{\mathbf{s}}[n] = \left(\hat{\mathbf{G}}[n]^{\mathrm{H}}\hat{\mathbf{G}}[n]\right)^{-1}\hat{\mathbf{G}}[n]^{\mathrm{H}}\mathbf{y}[n], \quad (9)$$

with matrix $\hat{\mathbf{G}}[n]$ being equal to $\hat{\mathbf{H}}[n]\,\mathbf{W}[n]$.

Applying a ZF equalizer, Equation (9) leads to the SINR on the m-th layer [8]

$$\gamma_m = \frac{\sigma_s^2}{(\sigma_n^2 + \sigma_e^2\sigma_{\mathrm{d}}^2)\,\mathbf{e}_m^{\mathrm{H}}\left(\hat{\mathbf{G}}[n]^{\mathrm{H}}\hat{\mathbf{G}}[n]\right)^{-1}\mathbf{e}_m}. \quad (10)$$

IV. Power Allocation

In this section, we show how to distribute the available power among data and pilot-symbols under flat and time-variant channels. Furthermore, we limit our discussion only to an Least Squares (LS) channel estimator. Note that based on the results shown in [8], all concepts can be easily applied also to any linear channel estimators.

A channel estimate at a data position $\hat{h}_{\mathrm{d},j}$ obtained via linear interpolation of the channel estimates at adjacent pilot positions can be mathematically expressed as

$$\hat{h}_{\mathrm{d},j} = \sum_{i\in\mathcal{P}_j} w_{j,i}\hat{h}_{\mathrm{p},i}, \quad (11)$$

where $\mathcal{P}_j$ represents the set of the adjacent pilot positions utilized for linear interpolation of the data-symbol located at a position j. The variable $w_{j,i}$ is a interpolation weight and it indicates how much a channel estimate at a position i influences channel estimate at a position j.

Every pilot-symbol pattern leads to a certain MSE of a channel estimator. In case of an LS channel estimator, the MSE can be stated as [8]

$$\sigma_e^2 = c_e(D)\,\frac{\sigma_n^2}{\sigma_{\mathrm{p}}^2} + d(D, f_d), \quad (12)$$

where $c_e(D)$ and $d(D, f_d)$ are real constants depending on the distance D between adjacent pilot-symbols that determine the performance of the channel estimators. The variable D denotes distance between two adjacent pilot-symbols. Clearly by increasing power at the pilot-symbols, MSE becomes smaller, but not smaller than the value of the variable $d(D, f_d)$. In [8] analytical expressions for $c_e(D)$ and $d(D, f_d)$ were derived as

$$c_e = \frac{1}{N_{\mathrm{d}}}\sum_{j=1}^{N_{\mathrm{d}}}\sum_{i\in\mathcal{P}_j} w_{j,i}^2, \quad (13)$$

and

$$d = \quad (14)$$

$$\frac{1}{N_{\mathrm{d}}}\sum_{j=1}^{N_{\mathrm{d}}}\left(1 - 2\sum_{i\in\mathcal{P}_j} w_{j,i}\Re\{R_{j,i}\} + \sum_{i\in\mathcal{P}_j}\sum_{i'\in\mathcal{P}_j} w_{j,i}w_{j,i'}R_{i,i'}\right),$$

where $R_{j,i}$ is a channel correlation coefficient between the j-th and the i-th channel positions.

Simplifying the SINR expression, we obtain:

$$\gamma_{m,k} = \frac{1}{N_{\mathrm{l}}\mathbf{e}_m^{\mathrm{H}}\left(\mathbf{G}[n]^{\mathrm{H}}\mathbf{G}[n]\right)^{-1}\mathbf{e}_m} f\left(\sigma_{\mathrm{p}}^2, \sigma_{\mathrm{d}}^2, D\right), \quad (15)$$

for which the power allocation function $f\left(p_{\text{off}}, D\right)$ is given as

$$f\left(\sigma_{\text{p}}^2, \sigma_{\text{d}}^2, D\right) = \frac{1}{\sigma_n^2 \left(\frac{1}{\sigma_{\text{d}}^2} + \frac{c_e(D)}{\sigma_{\text{p}}^2}\right) + d\left(D, f_d\right)}. \tag{16}$$

Note that the power allocation function is independent of the channel realization.

V. Pilot Design

In this section, we analyze pilot-symbol patterns using our post-equalization SINR framework. In general, certain amount of resources like bandwidth and power are available for transmission of data and pilot-symbols. If more resources are used for data transmission, there is less left for the transmission of the pilot-symbols, leading to a degradation of the channel estimation performance. Clearly, there is an equilibrium for the distribution of the available resources.

It has been shown that equidistant pilot-symbols are optimal in terms of capacity and MSE [1, 13]. Therefore, we consider equidistant pilot patterns with distance D between adjacent pilots. An example of such pattern is shown in Figure 1.

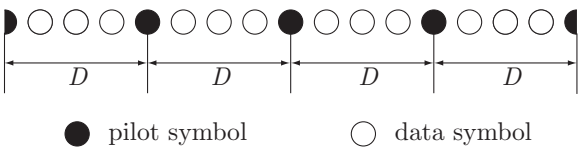

Fig. 1. Pilot pattern with equidistant reference symbols represented by black dots multiplexed within available resources with distance D.

The coefficient $c_e\left(D\right)$ from Equation (12) is purely determined by the pilot-symbol pattern and the coefficient $d\left(D, f_d\right)$ is additionally dependent on the maximum Doppler frequency. Figure 2 shows the behavior of these coefficients over distance between two adjacent pilot-symbols. Let us first consider $c_e\left(D\right)$. At low distances it grows rapidly with increasing distance between two pilot-symbols. At rather large distances, it remains almost constant. The value of the coefficient $d\left(D, f_d\right)$ strongly depends on the maximum Doppler frequency. For $f_d = 0\,\text{Hz}$, which corresponds to time-invariant case, the variable $d\left(D, f_d\right)$ is zero for all distance between pilot-symbols. In this case, the saturation effect of the channel estimator does not occur [8]. For non zero maximum Doppler frequencies, the value of $d\left(D, f_d\right)$ grows with increasing maximum Doppler frequency. The curves are however not monotone due to the assumed Jakes' spectrum with the autocorrelation function given by a Bessel function.

The optimal distance between two adjacent pilot-symbols and power distribution between pilot and data-symbols cannot be found exclusively by maximizing the post-equalization SINR. This would lead to a solution with a small distance between adjacent pilot-symbols, which would decrease the available bandwidth for data transmission [14]. Therefore, another type of a cost function is required which allows to include a penalty due to the bandwidth occupied by the pilot-symbols. The constrained channel capacity [15] is thus a natural choice for the new cost function

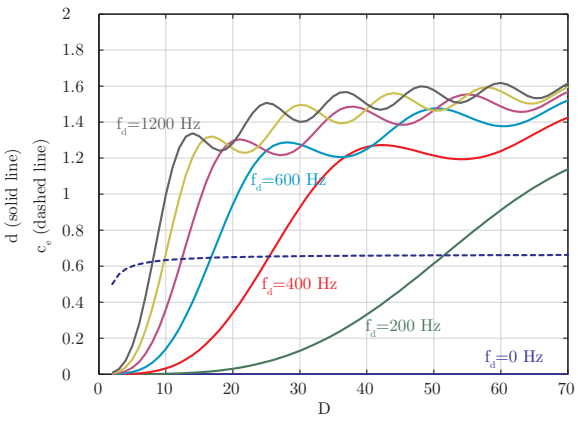

Fig. 2. Coefficients $c_e\left(D\right)$ and $d\left(D, f_d\right)$ over distance between two adjacent pilot-symbols for an LS channel estimator for various maximum Doppler frequencies.

$$\mathcal{C} = B\left(D\right) \log_2\left(1 + \gamma_m\right), \tag{17}$$

where B is the bandwidth utilized for the data transmission. Inserting the post-equalization SINR into the capacity expression allows to consider the effect of the channel estimation error and power allocation in a very simple way. The post-equalization SINR Equation (15) can be multiplicatively decomposed into two parts, the channel independent power allocation function Equation (16) and a function that depends on the actual channel $f_h\left(\mathbf{G}\left[n\right]\right) = \frac{1}{N_{\text{t}} \mathbf{e}_m^{\text{H}} \left(\mathbf{G}[n]^{\text{H}} \mathbf{G}[n]\right)^{-1} \mathbf{e}_m}$. In order to maximize the system's capacity without taking into account an actual channel realization, we approximate Equation (17) at high SNR by

$$\begin{aligned} \mathcal{C} &\approx B\left(D\right) \log_2\left(f\left(\sigma_{\text{p}}^2, \sigma_{\text{d}}^2, D\right) f_h\left(\mathbf{G}\left[n\right]\right)\right) \\ &\approx B\left(D\right) \log_2\left(f\left(\sigma_{\text{p}}^2, \sigma_{\text{d}}^2, D\right)\right) + B\left(D\right) \log_2\left(f_h\left(\mathbf{G}\left[n\right]\right)\right) \end{aligned} \tag{18}$$

and at low SNR by

$$\mathcal{C} \approx \log_2\left(e\right) B\left(D\right) f\left(\sigma_{\text{p}}^2, \sigma_{\text{d}}^2, D\right) f_h\left(\mathbf{G}\left[n\right]\right). \tag{19}$$

The only part influenced by changing the distance between pilots and by adjusting the power allocation is $B\left(D\right) \log_2\left(f\left(\sigma_{\text{p}}^2, \sigma_{\text{d}}^2, D\right)\right)$ for high SNR and $B\left(D\right) f\left(\sigma_{\text{p}}^2, \sigma_{\text{d}}^2, D\right)$ for low SNR values, respectively. Therefore, we define the cost function as

$$f_{\text{cost}}\left(\sigma_{\text{p}}^2, \sigma_{\text{d}}^2, D\right) = \begin{cases} B\left(D\right) f\left(p_{\text{off}}, D\right) & ;\text{SNR} < \text{SNR}_{\text{tr}} \\ B\left(D\right) \log_2\left(f\left(p_{\text{off}}, D\right)\right) & ;\text{SNR} > \text{SNR}_{\text{tr}} \end{cases} \tag{20}$$

where SNR_{tr} is an SNR threshold value, at which the capacity approximation for low SNR values is replaced by that at high SNR values. With the above defined cost function, we can

formulate our optimization problem as

$$\begin{aligned} \underset{\sigma_{\mathrm{p}}^2,\sigma_{\mathrm{d}}^2,D}{\text{maximize}} \quad & f_{\text{cost}}\left(\sigma_{\mathrm{p}}^2,\sigma_{\mathrm{d}}^2,D\right) \\ \text{subject to} \quad & N_{\mathrm{d}}\sigma_x^2 + N_{\mathrm{p}}\sigma_{\mathrm{p}}^2 = \text{const} \\ & \text{bandwidth} = \text{const} \end{aligned}$$

Since the optimization problem does not depend on the instantaneous channel realization, it can be straightforwardly solved offline.

Figure 3 shows optimal choice of the distance between adjacent pilot-symbols over SNR for various values of the maximum Doppler frequency. Two obvious trends can be observed from the plot

- With increasing maximum Doppler frequency, the optimal distance between adjacent pilot-symbols is decreasing.
- With increasing SNR, the optimal distance between adjacent pilot-symbols is decreasing.

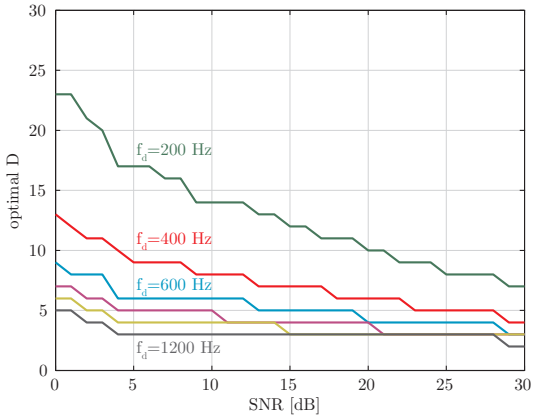

Fig. 3. Optimal choice of the distance between adjacent pilot-symbols D over SNR for alues of the maximum Doppler frequency f_D.

Figure 4 shows optimal choice of the ratio of the pilot power and data power $p_{\text{off}} = \frac{\sigma_{\mathrm{p}}^2}{\sigma_{\mathrm{d}}^2}$ over SNR for various values of the maximum Doppler frequency. Two obvious trends can be observed from the plot

- With increasing maximum Doppler frequency, the optimal power assigned to the pilot-symbols is decreasing.
- With increasing SNR, the optimal power assigned to the pilot-symbols is decreasing.

VI. Simulation Results

In this section, we present simulation results and compare the capacity of a system using an optimal distance between adjacent pilot-symbols and with an optimal power distribution between pilot and data-symbols, against a system using a fixed distance between pilot-symbols and an unit distribution of power among data and pilot-symbols. All data, tools and scripts are available online [10] in order to allow other researchers to reproduce the results shown in this paper. Table I shows the most important simulator settings.

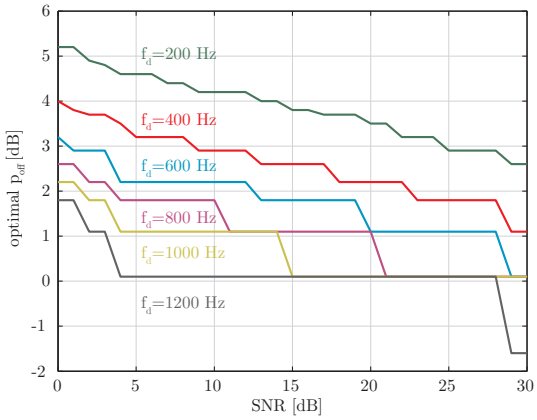

Fig. 4. Optimal choice of the ratio of the pilot power and data power $\frac{\sigma_{\mathrm{p}}^2}{\sigma_{\mathrm{d}}^2}$ over SNR for alues of the maximum Doppler frequency f_d.

TABLE I
Simulator settings for fast fading simulations

Parameter	Value
Number of transmit antennas	1
Number of receive antennas	1
Receiver type	ZF
Channel type	flat Rayleigh fading
Symbol duration (T_s)	$\frac{1}{14}$ ms
Carrier frequency (f_s)	2.5 GHz

We chose the symbol duration to be $T_s = \frac{1}{14}$ ms. This symbol duration is used also in Long Term Evolution (LTE). Capacities of two different systems are compared in Figure 5. The solid lines represent a system using the optimal distance between adjacent pilot-symbols and optimal power distribution between pilot- and data-symbols. The optimal values for both of the variables are shown in Figure 3 and Figure 4. The dashed line in Figure 5 represents a system using a fixed distance between adjacent pilot-symbols $D = 7$ and no power distribution between pilot and data-symbols. We chose $D = 7$, because this is the distance used in an LTE system [16].

VII. Conclusion

In this paper, we tackled the problem of optimal pilot-symbol design for time-variant scenarios. We delivered an analytical expressions for the optimal distance between adjacent pilot-symbols and the optimal power distribution between pilot-symbols and data-symbols. The optimal values were confirmed by means of simulations and compared to a system using a fixed distance between adjacent pilot-symbols and unit power distribution. Such a system is significantly outperformed by an optimal system in terms of capacity. In this paper, we showed that at low SNR values the number of necessary pilot-symbols can be decreased, but their power have to be significantly increased compared to the power of the data-symbols. On the other hand, at high SNR values, in order to an obtain optimal system performance, pilot-symbols pattern with higher density have to be utilized, though with smaller power offset.

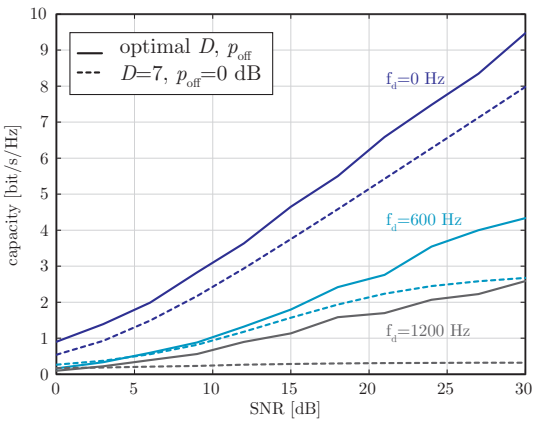

Fig. 5. Capacity versus SNR for system with optimal pilot distance D between pilot-symbols and optimal power offset p_{off} (solid line) and for system with fixed distance between pilot-symbols ($D = 7$) and no power distribution (dashed line).

ACKNOWLEDGMENTS

The authors would like to thank the LTE research group for continuous support and lively discussions. This work has been funded by the Christian Doppler Laboratory for Wireless Technologies for Sustainable Mobility, KATHREIN-Werke KG, and A1 Telekom Austria AG. The financial support by the Federal Ministry of Economy, Family and Youth and the National Foundation for Research, Technology and Development is gratefully acknowledged.

REFERENCES

[1] R. Negi and J. Cioffi, "Pilot Tone Selection for Channel Estimation in a Mobile OFDM System," *IEEE Transactions on Consumer Electronics*, vol. 44, no. 3, pp. 1122–1128, Aug. 1998.

[2] Jiann-Ching Guey, M.P. Fitz, M.R. Bell, and Wen-Yi Kuo, "Signal design for transmitter diversity wireless communication systems over Rayleigh fading channels," in *IEEE 46th Vehicular Technology Conference, 1996.*, May 1996, vol. 1, pp. 136 –140 vol.1.

[3] Min Dong, Lang Tong, and B.M. Sadler, "Optimal insertion of pilot symbols for transmissions over time-varying flat fading channels," *IEEE Transactions on Signal Processing*, vol. 52, no. 5, pp. 1403 – 1418, May 2004.

[4] Lang Tong, B.M. Sadler, and Min Dong, "Pilot-assisted wireless transmissions: general model, design criteria, and signal processing," *IEEE Signal Processing Magazine*, vol. 21, no. 6, pp. 12 – 25, Nov. 2004.

[5] I. Cosovic and G. Auer, "Capacity Achieving Pilot Design for MIMO-OFDM over Time-Varying Frequency-Selective Channels," in *IEEE International Conference on Communications*, June 2007, pp. 779 –784.

[6] M. Šimko, S. Pendl, S. Schwarz, Q. Wang, J. C. Ikuno, and M. Rupp, "Optimal Pilot Symbol Power Allocation in LTE," in *Proc. 74th IEEE Vehicular Technology Conference (VTC2011-Fall)*, San Francisco, USA, Sept. 2011.

[7] M. Šimko and M. Rupp, "Optimal Pilot Symbol Power Allocation in Multi-Cell Scenarios of LTE," in *Conference Record of the Fourtyfifth Asilomar Conference on Signals, Systems and Computers, 2011*, Pacific Grove, USA, Nov. 2011.

[8] M. Šimko, Q. Wang, and M. Rupp, "Optimal Pilot Symbol Power Allocation under Time-variant Channels," *EURASIP Journal on Wireless Communications and Networking*, 2012.

[9] M. Šimko, P. S. R. Diniz, Q. Wang, and M. Rupp, "Power Efficient Pilot Symbol Power Allocation under Time-variant Channels," in *Proc. 76th IEEE Vehicular Technology Conference (VTC2012-Fall)*, Quebec, Canada, Sept. 2012.

[10] "LTE simulator homepage," [online] http://www.nt.tuwien.ac.at/ltesimulator/.

[11] A. Hedayat, A. Nosratinia, and N. Al-Dhahir, "Linear Equalizers for Flat Rayleigh MIMO Channels," in *Proc. of IEEE ICASSP 2005*, Mar. 2005, vol. 3, pp. iii/445 – iii/448 Vol. 3.

[12] M. Rupp, "Robust Design of Adaptive Equalizers," *IEEE Transactions on Signal Processing*, vol. 60, no. 4, pp. 1612 –1626, Apr. 2012.

[13] I. Barhumi, G. Leus, and M. Moonen, "Optimal Training Design for MIMO OFDM Systems in Mobile Wireless Channels," *IEEE Transactions on Signal Processing*, vol. 51, no. 6, pp. 1615–1624, 2003.

[14] M. Šimko, P. S. R. Diniz, and M. Rupp, "Design Requirements of Adaptive Pilot-Symbol Patterns," in *Proc. of ICC Workshop Beyond LTE-A*, Budapest, Hungary, June 2013, submitted.

[15] S. Schwarz, M. Šimko, and M. Rupp, "On performance bounds for MIMO OFDM based wireless communication systems," in *Signal Processing Advances in Wireless Communications SPAWC 2011*, San Francisco, CA, June 2011, pp. 311 –315.

[16] 3GPP, "Evolved Universal Terrestrial Radio Access (E-UTRA); Physical channels and modulation," TS 36.211, 3rd Generation Partnership Project (3GPP), Sept. 2008.